Prevention of H5N6 outbreaks in the Philippines using optimal control

Abel G. Lucido*[1,2,3], Robert Smith?[4], and Angelyn R. Lao[2,3]

[1]Department of Science & Technology - Science Education Institute, Bicutan, Taguig, Philippines
[2]Mathematics and Statistics Department, De La Salle University, 2401 Taft Avenue, 0922 Manila, Philippines
[3]Center for Complexity and Emerging Technologies, De La Salle University, 2401 Taft Avenue, 0922 Manila,Philippines
[4]Department of Mathematics and Faculty of Medicine, University of Ottawa, 150 Louis-Pasteur Pvt Ottawa, ON K1N 6N5, Canada

Highly Pathogenic Avian Influenza A (H5N6) is a mutated virus of Influenza A (H5N1) and a new emerging infection that recently caused an outbreak in the Philippines. The 2017 H5N6 outbreak resulted in a depopulation of 667,184 domestic birds. We incorporate half-saturated incidence and optimal control in our mathematical models in order to investigate three intervention strategies against H5N6: isolation with treatment, vaccination, and modified culling. We determine the direction of the bifurcation when $R_0=1$ and show that all the models exhibit forward bifurcation. We apply the theory of optimal control and perform numerical simulations to compare the consequences and implementation cost of utilizing different intervention strategies in the poultry population. Despite the challenges of applying each control strategy, we show that culling both infected and susceptible birds is an effective control strategy in limiting an outbreak, with a consequence of losing a large number of birds; the isolation-treatment strategy has the potential to prevent an outbreak, but it highly depends on rapid isolation and successful treatment used; while vaccination alone is not enough to control the outbreak.

*Corresponding author
Email Address: abel_lucido@dlsu.edu.ph
Date received: February 28, 2020
Date revised: August 27, 2020
Date accepted: October 3, 2020

KEYWORDS

Influenza A (H5N6), half-saturated incidence, isolation-treatment, culling, vaccination, bifurcation, optimal control

1. INRODUCTION

Avian influenza is a highly contagious disease of birds caused by infection with influenza A viruses that circulate in domestic and wild birds (WHO 2020). Some avian influenza virus subtypes are H5N1, H7N9 and H5N6, which are classified according to combinations of different virus surface proteins hemagglutinin (HA) and neuraminidase (NA). This disease is categorized as either Highly Pathogenic Avian Influenza (HPAI), which causes severe disease in poultry and results in high death rates, or Low Pathogenic Avian Influenza (LPAI), which causes mild disease in poultry (WHO 2020).

As reported by the World Health Organization (WHO), H5N1 has been detected in poultry, wild birds and other animals in over 30 countries and has caused 861 human cases in 16 of these countries and 455 deaths. H5N6 was reported emerging from China in early May 2014 (Joob and Viroj 2015). H5N6 has replaced H5N1 as one of the dominant avian influenza virus subtypes in southern China (Bi *et al.* 2016). In August 2017, cases of H5N6 in the Philippines resulted in the culling of 667,184 chicken, ducks and quails (OIE 2020).

Due to the potential of avian influenza virus to cause a pandemic, several mathematical models have been developed in order to test control strategies. Several studies included saturation

incidence, where the rate of infection will eventually saturate, showing that protective measures have been put into place as the number of infected birds increases (Capasso and Serio 1978). With half-saturated incidence, it includes the half-saturation constant, which pertains to the density of infected individuals that yields 50% chance of contracting the disease (Shi *et al.* 2019). When half-saturated incidence is included, the effect is a significantly lower peak of the total number of infected humans compared to the case when half-saturated incidence is not included (Chong *et al.* 2013). However, when half-saturation is included, the disease takes longer to die off. We are thus using half-saturated incidence to investigate the effects of outbreaks that may have a long tail. Some intervention strategies employed to protect against avian influenza are biosecurity, quarantine, control in live markets, vaccination and culling.

Emergency vaccination, prophylactic or preventive vaccination, and routine vaccination are the three vaccination strategies mentioned by the United Nations Food and Agriculture Organization (UNFAO). In China, A(H5N1) influenza infection caused severe economic damage for the poultry industry, and vaccination served a significant role in controlling the spread of this infection since 2004 (Chen 2009). UNFAO and Office International des Epizooties (OIE) of the World Organization for Animal Health suggested vaccination of flocks should replace mass culling of poultry as the primary control strategy during outbreak (Butler 2005). For this reason, many mathematical models focus on how vaccination could prohibit the spread of infection.

Culling is a widely used control strategy during an outbreak of avian influenza virus (AIV). During the 2017 outbreak of H5N6 in the Philippines, mass culling was implemented to control the spread of AIV. Gulbudak and Martcheva (2013) suggested a modified culling strategy, which involves culling only the infected birds and high-risk in-contact birds. They utilized a function to represent the culling rate considering both HPAI and LPAI. Gulbudak *et al.* (2014) used half-saturated incidence to describe the culling of infected birds. The two-host model of Liu and Fang (2015) showed that screening and culling of infected poultry is a critical measure for preventing human A(H7N9) infections in the long term. There is a limited understanding of the effects of isolation with treatment as a control strategy to counter the spread of avian influenza. Isolation is also used when adding a new flock of birds to the poultry farm in order to prevent the possible transmission of disease to the current flock. The importance of optimal-control theory in modeling infectious diseases has been highlighted by several recent studies. Agusto (2013) used optimal control and cost-effective analysis in a two-strain avian influenza model. Jung *et al.* (2009) used optimal control in modeling H5N1 to prevent an influenza pandemic. Kim *et al.* (2018) utilized an optimal-control approach in modeling tuberculosis (TB) in the Philippines. Okosun and Smith? (2017) used optimal control to examine strategies for malaria–schistosomiasis coinfection.

To the best of our knowledge, optimal-control theory has not been applied to the spread of infectious diseases with transmission represented by half-saturated incidence. In this study, we adapt the vaccination model and modify the isolation model of Lee and Lao (2017). We modify the isolation model by partitioning the outflow of birds from isolation into two compartments. A proportion of birds will transfer to the recovered population, while the remainder will return to the infected population. We focus on the poultry population and use half-saturated incidence to describe the transmission of AIV. We include a modified culling strategy as one of our control strategies and use half-saturated incidence to depict the modified culling of susceptible and infected birds. We apply optimal-control theory to our three strategies — isolation-treatment, vaccination, and culling — and determine which among these strategies can inhibit the occurrence of an AIV outbreak.

2. THE MODELS

We examine three control strategies: isolation-treatment, culling, and vaccination. Our mathematical models are in the form of half-saturated incidence (HSI), which takes into consideration the density of infected individuals in the population that yields 50% chance of contracting avian influenza. Mathematical models with half-saturated incidence are more realistic compared to models with bilinear incidence (Chong *et al.* 2013, Lee and Lao 2018). We present four mathematical models: a model without control, which describes the transmission dynamics of avian influenza in bird population (i.e., the AIV model), and three models obtained by applying the following intervention strategies: isolation with treatment, vaccination, and culling. Description of variables and parameters used in the models are listed in the table in Appendix A.

2.1. AIV model without intervention

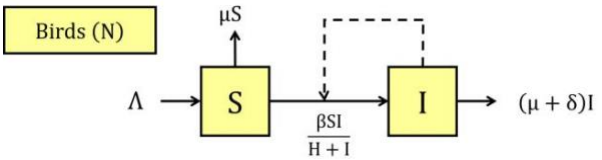

Figure 1: Schematic diagram of the AIV model with half-saturated incidence.

In the AIV model without intervention (shown in Figure 1) the bird population is divided into subpopulations (represented by compartments): susceptible birds (S) and infected birds (I). The total bird population is represented by $N(t)$ at time t, where $N(t) = S(t) + I(t)$. The number of susceptible birds increases through the birth rate (Λ) and reduces through the natural death rate of birds (μ) which are both constant parameter values. Infected birds additionally decrease through the disease-specific death rate (δ).

The number of susceptible birds who become infected through direct contact is represented by $\frac{\beta SI}{H+I}$, which denotes the transfer of the susceptible bird population to the infected bird population. Note that β is the rate of transmitting AIV and H is the half-saturation constant, indicating the density of infected individuals in the population that yields 50% possibility of contracting avian influenza (Chong *et al.* 2013). The saturation effect of the infected bird population indicates that a very large number of infected may tend to reduce the number of contacts per unit of time due to awareness of farmers to the disease (Capasso and Serio 1978). In Figure 1, the dashed directional arrow from I to the arrow from S to I indicates that $\frac{\beta SI}{H+I}$ is regulated by I.

Based on the AIV model described above, we have the following system of nonlinear ordinary differential equations (ODEs):

$$\begin{aligned} \dot{S} &= \Lambda - \frac{\beta SI}{H+I} - \mu S, \\ \dot{I} &= \frac{\beta SI}{H+I} - (\mu + \delta) I. \end{aligned} \tag{1}$$

2.2. Confinement with treatment strategy for infected poultry (isolation-treatment model)

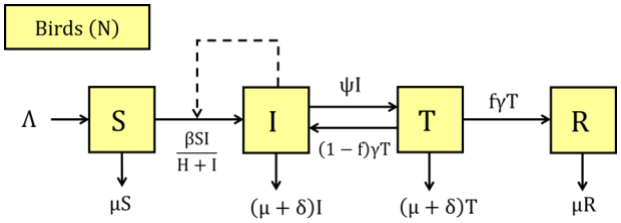

Figure 2: Schematic diagram of isolation-treatment model with HSI.

Here, we employ the strategy of confining and treating the infected poultry population (which will be referred as the isolation-treatment strategy). Several studies concluded that reducing the contact rate is an effective measure in preventing the spread of infection into the population (Lee and Lao 2018, Teng et al. 2018). For the isolation-treatment model (shown in Figure 2), we have included the compartment representing the population of isolated birds that undergoes treatment (T) and the compartment representing the population of recovered birds (R). We denote the isolation rate of identified infected birds by ψ and the release rate of birds from isolation by γ.

During isolation, we apply treatment then release birds afterward. These birds will either recover successfully (transfer to recovered population) or remain infected (return to the infected population) depending on the effectiveness of treatment. The proportion of isolated birds that have recovered is represented by f, while the proportion of isolated birds that have not recovered (and so remained infected) are represented by (1-f). We did not consider natural recovery of poultry in our model, due to the high mortality rate of HPAI virus infection.

The system of ODEs for the isolation-treatment model is

$$\begin{aligned} \dot{S} &= \Lambda - \frac{\beta SI}{H+I} - \mu S, \\ \dot{I} &= \frac{\beta SI}{H+I} + (1-f)\gamma T - (\mu + \delta + \psi)I, \\ \dot{T} &= \psi I - (\mu + \delta + \gamma)T, \\ \dot{R} &= f\gamma T - \mu R. \end{aligned} \tag{2}$$

2.3. Immunization of the poultry population (vaccination model)

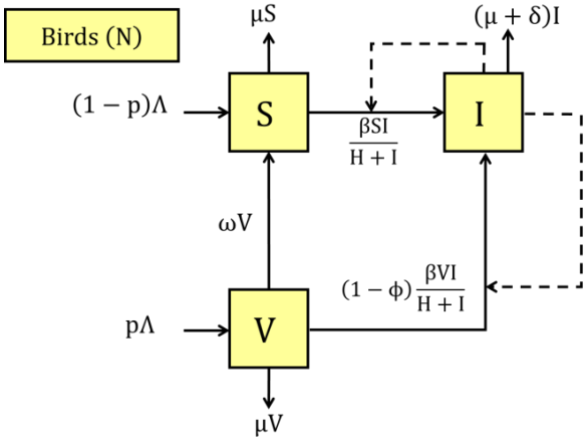

Figure 3: Schematic diagram of preventive vaccination model with HSI.

We modified the vaccination model of Lee and Lao (2018) by splitting the birth rate (Λ) depending on the proportion of vaccinated population (p), as shown in Figure 3. The poultry population prone to H5N6 is divided into two compartments: vaccinated birds represented by V and susceptible, unvaccinated birds denoted by S. In our vaccination model, we differentiate the immunized group (vaccinated) from non-immunized group (unvaccinated).

We investigate the effectiveness of the vaccine not only through its reported efficacy (denoted by ϕ) but also based on the waning rate of the vaccine (denoted by ω). To represent the acquired immunity of the vaccinated group, the infectivity of vaccinated birds is reduced by a factor $(1-\phi)$. The system of ODEs representing the vaccination model is

$$\begin{aligned} \dot{S} &= (1-p)\Lambda + \omega V - \frac{\beta SI}{H+I} - \mu S, \\ \dot{V} &= p\Lambda - (1-\phi)\frac{\beta VI}{H+I} - (\mu + \omega)V, \\ \dot{I} &= \frac{\beta SI}{H+I} + (1-\phi)\frac{\beta VI}{H+i} - (\mu + \delta)I. \end{aligned} \tag{3}$$

2.4. Depopulation of susceptible and infected birds (culling model)

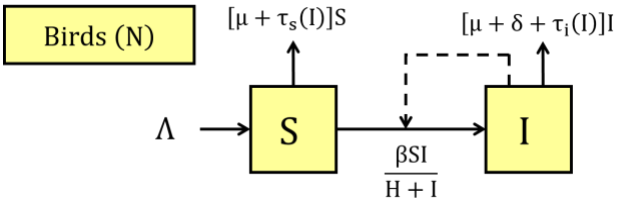

Figure 4: Schematic diagram of depopulation or culling model with HSI.

We modified the culling model of Gulbudak *et al.* (2014) by incorporating the dynamics of half-saturated incidence on the transmission of infection and on the culling rate for infected birds and for susceptible birds that are at high risk of infection. We define the culling function of the infected and susceptible birds as $\tau_i = \frac{c_i I}{H+I}$ and $\tau_s = \frac{c_s I}{H+I}$, respectively. The culling frequency is represented by c_s for susceptible birds and c_i for infected birds. The following system of ODEs represents the culling model:

$$\begin{aligned} \dot{S} &= \Lambda - \frac{\beta SI}{H+I} - \tau_s(I)S - \mu S, \\ \dot{I} &= \frac{\beta SI}{H+I} - \tau_i(I)I - (\mu + \delta)I. \end{aligned} \tag{4}$$

3. STABILITY AND BIFURCATION ANALYSIS

We first analyze the AIV model without intervention. The disease-free equilibrium (DFE) of the AIV model (1) is

$$E_A^0 = (S^0, I^0) = \left(\frac{\Lambda}{\mu}, 0\right).$$

We denote the basic reproduction number as $\mathcal{R}_A$ for the AIV model and obtain

$$\mathcal{R}_A = \frac{\beta\Lambda}{H\mu(\mu+\delta)}. \tag{5}$$

The DFE E_A^0 of the AIV model is locally asymptotically stable if $\mathcal{R}_A < 1$ and unstable if $\mathcal{R}_A > 1$.

The endemic equilibrium for the AIV model is represented by

$$E_A^* = (S^*, I^*) = \left(\frac{\Lambda + H(\mu+\delta)}{\mu+\beta}, \frac{\beta\Lambda - \mu H(\mu+\delta)}{(\mu+\delta)(\mu+\beta)}\right). \tag{6}$$

We can rewrite I^* as

$$I^* = \frac{\mu H}{\mu + \beta}(\mathcal{R}_A - 1).$$

When $\mathcal{R}_A \leq 1$, it follows that $I^* \leq 0$, so there is no biologically feasible endemic equilibrium. For $\mathcal{R}_A > 1$, we have $I^* > 0$, so we have an endemic equilibrium. We conclude that the AIV model has no endemic equilibrium when $\mathcal{R}_A \leq 1$, and has an endemic equilibrium when $\mathcal{R}_A > 1$. It follows that reducing the basic reproduction number $\mathcal{R}_A$ below one is sufficient to eliminate avian influenza from the poultry population.

As exhibited in Figure 5A, we have a bifurcation plot between the infected population and the basic reproduction number $\mathcal{R}_A$. When the basic reproduction number is below one and the DFE and the endemic equilibrium coexist, then we have a backward bifurcation. A forward bifurcation is when the basic reproduction number crosses one from below and the DFE becomes unstable while the endemic equilibrium becomes stable. Clearly, we have a forward bifurcation for the AIV model, showing that when the basic reproduction number crosses unity, an endemic equilibrium appears and the DFE continues to exist but loses its stability.

We continue by investigating different strategies that can reduce or stop the spread of AIV. From the isolation-treatment model (2), the DFE is given by

$$E_{\mathrm{T}}^0 = (S^0, I^0, T^0, R^0) = \left(\frac{\Lambda}{\mu}, 0, 0, 0\right).$$

The corresponding basic reproduction number $(\mathcal{R}_T)$ with respect to (2) is represented by

$$\mathcal{R}_T = \frac{\beta\Lambda(\mu + \delta + \gamma)}{H\mu[(\mu + \delta + \psi)(\mu + \delta + \gamma) - (1 - f)\gamma\psi]}. \quad (7)$$

The DFE (E_T^0) of the isolation-treatment model is locally asymptotically stable if $\mathcal{R}_T < 1$ and unstable if $\mathcal{R}_T > 1$. Consequently, we can identify some conditions on how confinement of infected birds affects the stability of E_T^0. The DFE (E_T^0) is locally asymptotically stable whenever

$$\frac{\beta\Lambda(\mu + \delta + \gamma) - H\mu(\mu + \delta)(\mu + \delta + \gamma)}{H\mu(\mu + \delta + f\gamma)} < \psi.$$

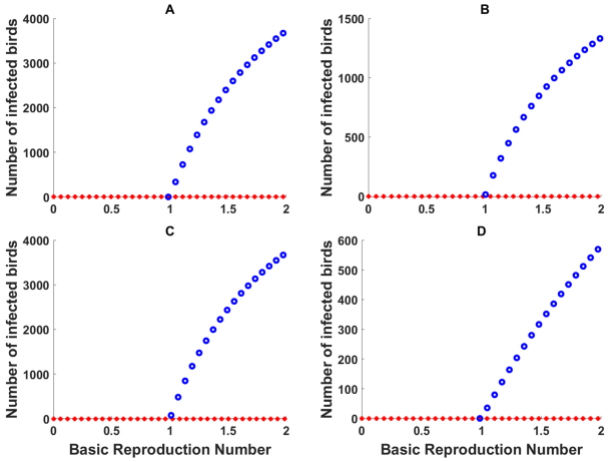

Figure 5: Bifurcation diagram for the basic reproduction number for AIV, considering no control (A), isolation-treatment (B), vaccination (C) and culling (D). Only forward bifurcations occur. Note the change of scale on the vertical axis in each case. The red dotted curve illustrates the unstable branch of the bifurcation diagram.

For the endemic equilibrium of the isolation-treatment model (2), we indicate the presence of infection in the population by letting $I_{\mathrm{T}}^* \neq 0$ and solve for S_{T}^*, I_{T}^*, T_T^*, and R_T^*. Thus, we have

$$E_{\mathrm{T}}^* = (S_{\mathrm{T}}^*, I_{\mathrm{T}}^*, T_T^* R_T^*) = \left(\frac{\Lambda(H + I_{\mathrm{T}}^*)}{\mu(H + I_{\mathrm{T}}^*) + \beta I_{\mathrm{T}}^*}, I_{\mathrm{T}}^*, \frac{\psi I_{\mathrm{T}}^*}{\mu + \delta + \gamma}, \frac{f\gamma\psi I_{\mathrm{T}}^*}{\mu + \delta + \gamma}\right), \quad (8)$$

where

$$I_{\mathrm{T}}^* = \frac{(\mu + \delta + \gamma)[\beta\Lambda - \mu H(\mu + \delta + \psi)] + (1 - f)\gamma\psi\mu H}{(\mu + \beta)[(\mu + \delta + \psi)(\mu + \delta + \gamma) - (1 - f)\gamma\psi]}.$$

Given the basic reproduction number (7), we rewrite the expression I_{T}^* of the isolation-treatment model as

$$I_{\mathrm{T}}^* = \frac{\mu H}{\mu + \beta}(\mathcal{R}_T - 1). \quad (9)$$

From (9), it follows that when $\mathcal{R}_T \leq 1$, we have $I_{\mathrm{T}}^* \leq 0$ and there is no endemic equilibrium; however, when $\mathcal{R}_T > 1$, we have $I_{\mathrm{T}}^* > 0$ and we have an endemic equilibrium. Thus, the isolation-treatment model (2) has no endemic equilibrium when $\mathcal{R}_T \leq 1$ and has an endemic equilibrium when $\mathcal{R}_T > 1$. Hence there is no backward bifurcation for the isolation-treatment model when $\mathcal{R}_T < 1$.

In Figure 5B, we have a forward bifurcation for the isolation-treatment model, which supports our claim. The bifurcation plot between the infected population I_{T}^* and the basic reproduction number $\mathcal{R}_T$ for the isolation-treatment model shows that reducing $\mathcal{R}_T$ below unity is enough to eliminate avian influenza from the poultry population.

Next, we analyze the stability of the associated equilibria of the AIV model with vaccination strategy (3). The DFE and the basic reproduction number are

$$E_V^0 = (S^0, V^0, I^0) = \left(\frac{\Lambda(\mu + \omega - p\mu)}{\mu(\mu + \omega)}, \frac{p\Lambda}{\mu + \omega}, 0\right)$$

and

$$\mathcal{R}_V = \frac{\beta\Lambda(\mu + \omega - p\mu\phi)}{\mu H(\mu + \omega)(\mu + \delta)}.$$

The DFE E_V^0 of vaccination model is locally asymptotically stable if $\mathcal{R}_V < 1$ and unstable if $\mathcal{R}_V > 1$. Moreover, we obtain some conditions for the proportion of vaccinated poultry (p) and vaccine efficacy (ϕ), which both range from 0 to 1. E_V^0 is locally asymptotically stable whenever

$$\left(\frac{\mu + \omega}{\mu}\right)\left(1 - \frac{\mu H(\mu + \delta)}{\Lambda\beta}\right) \leq p\phi < 1.$$

For the endemic equilibrium of the vaccination model (3), we obtain the following:

$$E_{\mathrm{V}}^* = (S_{\mathrm{V}}^*, V_{\mathrm{V}}^*, I_V^*), \quad (10)$$

where

$$S_{\mathrm{V}}^* = \frac{(H + I_V^*)[(1 - p)\Lambda[(H + I_V^*)(\mu + \omega) + (1 - \phi)\beta I_V^*] + \omega p\Lambda(\mathrm{H} + I_V^*)]}{[\mu(H + I_V^*) + \beta I_V^*][(H + I_V^*)(\mu + \omega) + (1 - \phi)\beta I_V^*]}$$

$$V_{\mathrm{V}}^* = \frac{p\Lambda(H + I_V^*)}{(H + I_V^*)(\mu + \omega) + (1 - \phi)\beta I_V^*}$$

$$I_V^* = \frac{-b \pm \sqrt{b^2 - 4ac}}{2a},$$

such that

$$a = -(\mu + \delta)[\mu\beta(1-\phi) + (\mu+\omega)(\mu+\beta) + \beta^2(1-\phi)],$$
$$b = \beta^2\Lambda(1-\phi) + \mu H(\mu+\delta)(\mu+\omega)(\mathcal{R}_V - 1) - H(\mu+\delta)[\mu\beta(1-\phi) + (\mu+\beta)(\mu+\omega)],$$
$$c = \mu H^2(\mu+\delta)(\mu+\omega)(\mathcal{R}_V - 1).$$

The vaccination model (3) has no endemic equilibrium when $\mathcal{R}_V \leq 1$, and has a unique endemic equilibrium when $\mathcal{R}_V > 1$. Figure 5C illustrates a bifurcation plot between the population of infected birds and the basic reproduction number $\mathcal{R}_V$, showing a forward bifurcation. This bifurcation diagram is in line with our result in Theorem B.1 in Appendix B, so there is no endemic equilibrium when $\mathcal{R}_V < 1$ but there is a unique endemic equilibrium when $\mathcal{R}_V > 1$. In this case, reducing $\mathcal{R}_V$ below one is sufficient to control the disease.

Finally, we analyze the stability of equilibria of the AIV model with culling (4). The DFE for the culling model is given by

$$E_C^0 = (S^0, I^0) = \left(\frac{\Lambda}{\mu}, 0\right),$$

and the basic reproduction number is

$$\mathcal{R}_C = \frac{\beta\Lambda}{\mu H(\mu+\delta)}.$$

The endemic equilibria of the culling model is determined as

$$E_C^* = (S_C^*, I_C^*) = \left(\frac{\Lambda(H + I_C^*)}{\mu H + (\mu + c_s + \beta)I_C^*}, I_C^*\right) \quad (11)$$

where $I_C^* = \frac{-b \pm \sqrt{b^2 - 4ac}}{2a}$,

such that

$$a = -(\mu + \delta + c_i)(\mu + c_s + \beta),$$
$$b = \mu H(\mu+\delta)(\mathcal{R}_C - 1) - c_i\mu H - H(\mu+\delta)(\mu + c_s + \beta),$$
$$c = \mu H^2(\mu+\delta)(\mathcal{R}_C - 1).$$

For the culling model (4), we have shown that a backward bifurcation does not exist when $\mathcal{R}_C < 1$. Thus, the culling model (4) has no endemic equilibrium when $\mathcal{R}_C < 1$, and has a unique endemic equilibrium when $\mathcal{R}_C > 1$.

In Figure 5D, we have a bifurcation diagram showing the infected population and the basic reproduction number $(\mathcal{R}_C)$. We have a forward bifurcation in the plot, which is similar to the result stated in Theorem B.2, implying that, when $\mathcal{R}_C < 1$, avian influenza will be eradicated from the poultry population.

4. OPTIMAL-CONTROL STRATEGIES

We now integrate an optimal-control approach in all our models: isolation-treatment, vaccination, and culling.

4.1. Isolation-treatment strategy

In applying the isolation-treatment strategy, we identify infected birds and isolate them at rate ψ. While the birds are isolated, we apply treatment such that a proportion f will successfully recover. Our first control involves isolating infected birds with u_1 replacing ψ. The second control indicates the effort of the farmers in choosing a drug that can increase the success of treatment with u_2 replacing f. The isolation-treatment model (2) becomes

$$\dot{S} = \Lambda - \frac{\beta SI}{H+I} - \mu S,$$
$$\dot{I} = \frac{\beta SI}{H+I} + (1 - u_2(t))\gamma T - (\mu + \delta + u_1(t))I,$$
$$\dot{T} = u_1(t)I - (\mu + \delta + \gamma)T,$$
$$\dot{R} = u_2(t)\gamma T - \mu R.$$

We represent the rate of isolation of infected birds by control $u_1(t)$ that is the rate $u_1(t)I$ transfers from I to T. The proportion of successfully treated birds released from isolation is denoted by $u_2(t)$.

The problem is to minimize the objective functional defined by

$$J_I(u_1, u_2) = \int_0^{t_f} \left[I(t) + T(t) + \frac{B_1}{2}u_1^2(t) + \frac{B_2}{2}u_2^2(t)\right] dt,$$

which is subject to the ordinary differential equations in (12) and where t_f is the final time. The objective functional includes isolation control $(u_1(t))$ and treatment control $(u_2(t))$, while B_1 and B_2 are weight constants associated with relative costs of applying respective control strategies. The quadratic formulation of the objective functional $J_I(u_1, u_2)$ is popular and useful to satisfy the convexity property of the cost function (Agusto 2013, Jung *et al.* 2009, Kim *et al.* 2018). Given that we have two controls $u_1(t)$ and $u_2(t)$, we want to find the optimal controls $u_1^*(t)$ and $u_2^*(t)$ such that

$$J_I(u_1^*, u_2^*) = \min_{\mathcal{U}_I}\{J_I(u_1, u_2)\},$$

where

$\mathcal{U}_I = \{(u_1, u_2) | u_i : [0, t_f] \to [a_i, b_i], i = 1,2, \text{is Lebesgue integrable}\}$ is the control set. We consider the best- and worst-case scenarios of isolating infected birds and giving treatment by setting the lower bounds to $a_i = 0$ and upper bounds to $b_i = 1$, for $i = 1,2$.

4.1.1. Characterization of optimal control for isolation-treatment strategy

We generate the necessary conditions of this optimal control using Pontryagin's Maximum Principle (Pontryagin *et al.* 1986). The Hamiltonian is

$$H_I = I(t) + T(t) + \frac{B_1}{2}u_1^2(t) + \frac{B_2}{2}u_2^2(t) + \lambda_{I_1}\left(\Lambda - \frac{\beta SI}{H+I} - \mu S\right) + \lambda_{I_2}\left(\frac{\beta SI}{H+I} + (1 - u_2(t))\gamma T - [\mu + \delta + u_1(t)]I\right) + \lambda_{I_3}(u_1(t)I - (\mu + \delta + \gamma)T) + \lambda_{I_4}(u_2(t)\gamma T - \mu R), \quad (13)$$

where $\lambda_{I_1}, \lambda_{I_2}, \lambda_{I_3}, \lambda_{I_4}$ are the associated adjoints for the states S, I, T, R. We obtain the system of adjoint equations by using the partial derivatives of the Hamiltonian (13) with respect to each state variable.

Theorem 4.1. There exist optimal controls $u_1^*(t)$and $u_2^*(t)$ and solutions S^*, I^*, T^*, R^* of the corresponding state system (12) that minimizes the objective functional $J_I(u_1, u_2)$ over $\mathcal{U}_I$. Since these optimal solutions exist, there exists adjoint variables $\lambda_{I_1}, \lambda_{I_2}, \lambda_{I_3}$ and λ_{I_4} satisfying

$$\dot{\lambda_{I_1}} = \lambda_{I_1}\left(\mu + \frac{\beta I}{H+I}\right) - \lambda_{I_2}\left(\frac{\beta I}{H+I}\right),$$

$$\dot{\lambda_{I_2}} = -1 + \lambda_{I_1}\left[\frac{H\beta S}{(H+I)^2}\right] - \lambda_{I_2}\left[\frac{H\beta S}{(H+I)^2}\right] + \lambda_{I_2}[\mu + \delta + u_1(t)] - \lambda_{I_3}u_1(t),$$
$$\dot{\lambda_{I_3}} = -1 - \lambda_{I_2}[1 - u_2(t)]\gamma + \lambda_{I_3}(\mu + \delta + \gamma) - \lambda_{I_4}u_2(t)\gamma,$$
$$\dot{\lambda_{I_4}} = \lambda_{I_4}\mu,$$

with transversality conditions $\lambda_{I_i}(t_f) = 0$, for $i = 1,2,3,4$. Furthermore,

$$u_1^* = \min\left\{b_1, \max\left\{a_1, \frac{(\lambda_{I_2} - \lambda_{I_3})I}{B_1}\right\}\right\} \text{ and}$$
$$u_2^* = \min\left\{b_2, \max\left\{a_2, \frac{(\lambda_{I_2} - \lambda_{I_4})\gamma T}{B_2}\right\}\right\}.$$

Proof. The existence of optimal control (u_1^*, u_2^*) is given by the result of Fleming and Rishel (1975). Boundedness of the solution of our system (2) shows the existence of a solution for the system. We have nonnegative values for the controls and state variables. In our minimizing problem, we have a convex integrand for J_I with respect to (u_1, u_2). By definition, the control set is closed, convex and compact, which shows the existence of optimality solutions in our optimal system. By Pontryagin's Maximum Principle, we obtain the adjoint equations and transversality conditions. We differentiate the Hamiltonian (13) with respect to the corresponding state variables as follows:

$$\frac{d\lambda_{I_1}}{dt} = -\frac{\partial H_I}{\partial S}, \frac{d\lambda_{I_2}}{dt} = -\frac{\partial H_I}{\partial I}, \frac{d\lambda_{I_3}}{dt} = -\frac{\partial H_I}{\partial T}, \frac{d\lambda_{I_4}}{dt} = -\frac{\partial H_I}{\partial R},$$

with $\lambda_{I_i}(t_f) = 0$ where $i = 1,2,3,4$. We consider the optimality condition

$$\frac{\partial H_I}{\partial u_1} = B_1 u_1(t) - \lambda_{I_2} I + \lambda_{I_3} I = 0 \text{ and}$$
$$\frac{\partial H_I}{\partial u_2} = B_2 u_2(t) - \lambda_{I_2}\gamma T + \lambda_{I_4}\gamma T = 0,$$

to derive the optimal controls in (14). We consider the bounds of the controls and obtain the characterization for optimal controls as follows:

$$u_1^* = \min\left\{1, \max\left\{0, \frac{(\lambda_{I_2} - \lambda_{I_3})I}{B_1}\right\}\right\} \text{ and}$$
$$u_2^* = \min\left\{1, \max\left\{0, \frac{(\lambda_{I_2} - \lambda_{I_4})\gamma T}{B_2}\right\}\right\}.$$

4.2. Vaccination

For vaccination, the first control represents the effort of the farmers to increase vaccinated birds, while the other control describes the efficacy of the vaccine in providing immunity against H5N6. $u_3(t)$ and $u_4(t)$ replace p and ϕ, respectively, in the vaccination model (3) to obtain

$$\begin{aligned} \dot{S} &= (1 - u_3(t))\Lambda + \omega V - \frac{\beta SI}{H + I} - \mu S, \\ \dot{V} &= u_3(t)\Lambda - (1 - u_4(t))\frac{\beta VI}{H + I} - (\mu + \omega)V, \\ \dot{I} &= \frac{\beta SI}{H + I} + (1 - u_4(t))\frac{\beta VI}{H + i} - (\mu + \delta)I. \end{aligned} \quad (15)$$

We describe the proportion of birds that are vaccinated by the control $u_3(t)$ and the immunity of the vaccinated population against acquiring the disease by $u_4(t)$. We have the objective functional

$$J_V(u_3, u_4) = \int_0^{t_f} \left[I(t) + \frac{B_3}{2}u_3^2(t) + \frac{B_4}{2}u_4^2(t)\right] dt,$$

which is subject to (15). This objective functional involves increased vaccination $u_3(t)$ and the vaccine-efficacy control $u_4(t)$, where B_3 and B_4 are the weight constants representing the relative cost of implementing each respective control. We need to find the optimal controls $u_3^*(t)$ and $u_4^*(t)$ such that

$$J_V(u_3^*, u_4^*) = \min_{\mathcal{U}_V}\{J_V(u_3, u_4)\},$$

where

$$\mathcal{U}_V = \{(u_3, u_4) | u_i : [0, t_f] \to [a_i, b_i], \quad i = 3,4, \text{is Lebesgue integrable}\}$$

is the control set. We consider the lower bound $a_i = 0$ and upper bounds $b_i = 1$, for $i = 3,4$.

4.2.1. Characterization of optimal control for vaccination strategy

In this case, the Hamiltonian is

$$\begin{aligned} H_V = I(t) &+ \frac{B_3}{2}u_3^2(t) + \frac{B_4}{2}u_4^2(t) \\ &+ \lambda_{V_1}\left((1 - u_3(t))\Lambda + \omega V - \mu S - \frac{\beta SI}{H + I}\right) \\ &+ \lambda_{V_2}\left(u_3(t)\Lambda - (\mu + \omega)V - (1 - u_4(t))\frac{\beta VI}{H + I}\right) \\ &+ \lambda_{V_3}\left(\frac{\beta SI}{H + I} + (1 - u_4(t))\frac{\beta VI}{H + I} - (\mu + \delta)I\right). \end{aligned} \quad (16)$$

Theorem 4.2. There exist optimal controls $u_3^*(t)$ and $u_4^*(t)$ and solutions S^*, V^*, I^* of the corresponding state system (15) that minimize the objective functional $J_V(u_3, u_4)$ over $\mathcal{U}_V$. Since these are optimal solutions, there exists adjoint variables $\lambda_{V_1}, \lambda_{V_2}$ and λ_{V_3} satisfying

$$\begin{aligned} \dot{\lambda_{V_1}} &= \lambda_{V_1}\left(\mu + \frac{\beta I}{H + I}\right) - \lambda_{V_3}\left(\frac{\beta I}{H + I}\right), \\ \dot{\lambda_{V_2}} &= -\lambda_{V_1}\omega + \lambda_{V_2}\left(\mu + \omega + (1 - u_4(t))\frac{\beta I}{H + I}\right) \\ &\quad - \lambda_{V_3}(1 - u_4(t))\frac{\beta I}{H + I}, \\ \dot{\lambda_{V_3}} &= -1 + \lambda_{V_1}\left[\frac{H\beta S}{(H + I)^2}\right] + \lambda_{V_2}\left[(1 - u_4(t))\frac{H\beta V}{(H + I)^2}\right] \\ &\quad - \lambda_{V_3}\left[\frac{H\beta S}{(H + I)^2} + (1 - u_4(t))\frac{H\beta V}{(H + I)^2}\right. \\ &\quad \left. - (\mu + \delta)\right], \end{aligned}$$

with transversality conditions $\lambda_{V_i}(t_f) = 0$, for $i = 1,2,3$. Furthermore,

$$u_3^* = \min\left\{b_3, \max\left\{a_3, \frac{(\lambda_{V_1} - \lambda_{V_2})\Lambda}{B_3}\right\}\right\} \text{ and}$$
$$u_4^* = \min\left\{b_4, \max\left\{a_4, \frac{(\lambda_{V_3} - \lambda_{V_2})\beta VI}{B_4(H + I)}\right\}\right\}. \quad (17)$$

The proof is similar to the proof of Theorem 4.1 and can be found in Appendix C.

4.3. Culling

Finally, we administer optimal control to the culling model (4). Thus, we have

$$\begin{aligned} \dot{S} &= \Lambda - \frac{\beta SI}{H + I} - \frac{u_5(t)SI}{H + I} - \mu S, \\ \dot{I} &= \frac{\beta SI}{H + I} - \frac{u_6(t)I^2}{H + I} - (\mu + \delta)I. \end{aligned} \quad (18)$$

We represent the frequency of culling the susceptible population by $u_5(t)$ and frequency of culling the infected population by $u_6(t)$. We have the objective functional

$$J_C(u_5, u_6) = \int_0^{t_f} \left[I(t) + \frac{B_5}{2} u_5^2(t) + \frac{B_6}{2} u_6^2(t) \right] dt,$$

which is subject to (18). The objective functional includes the susceptible and infected culling control denoted by $u_5(t)$ and $u_6(t)$, respectively, with B_5 and B_6 as the weight constants representing the relative cost of implementing each respective control. Hence we have to find the optimal controls u_5^* and u_6^* such that

$$J_C(u_5^*, u_6^*) = \min_{\mathcal{U}_C} \{J_C(u_5, u_6)\},$$

where

$$\mathcal{U}_C = \{(u_5, u_6) | u_i : [0, t_f] \to [a_i, b_i], \quad i = 5,6, \text{is Lebesgue integrable}\}$$

is the control set. We consider the lower bound $a_i = 0$ and upper bounds $b_i = 1$, for $i = 5, 6$.

4.3.1. Characterization of optimal control for culling strategy

In this case, the Hamiltonian is

$$\begin{aligned} H_C = I(t) + \frac{B_5}{2} u_5^2(t) + \frac{B_6}{2} u_6^2(t) \\ + \lambda_{C_1} \left(\Lambda - \mu S - \frac{u_5(t) SI}{H + I} - \frac{\beta SI}{H + I} \right) \\ + \lambda_{C_2} \left(\frac{\beta SI}{H + I} - (\mu + \delta) I - \frac{u_6(t) I^2}{H + I} \right). \end{aligned} \quad (19)$$

Theorem 4.3. There exists optimal controls $u_5^*(t)$ and $u_6^*(t)$ and solutions S^*, I^* of the corresponding state system (18) that minimize the objective functional $J_C(u_5, u_6)$ over $\mathcal{U}_C$. Since these optimal solutions, there exists adjoint variables λ_{C_1} and λ_{C_2}satisfying

$$\begin{aligned} \dot{\lambda_{C_1}} &= \lambda_{C_1} \left(\mu + \frac{u_5(t) I}{H + I} + \frac{\beta I}{H + I} \right) - \lambda_{C_2} \left(\frac{\beta I}{H + I} \right), \\ \dot{\lambda_{C_2}} &= -1 + \lambda_{C_1} \left(\frac{u_5(t) HS}{(H + I)^2} + \frac{H \beta S}{(H + I)^2} \right) \\ &\quad - \lambda_{C_2} \left(\frac{H \beta S}{(H + I)^2} - (\mu + \delta) \right. \\ &\quad \left. - \frac{(2H + I) u_6(t) I}{(H + I)^2} \right), \end{aligned}$$

with transversality conditions $\lambda_{C_i}(t_f)$, for $i = 1, 2$. Furthermore,

$$\begin{aligned} u_5^* &= \min \left\{ b_5, \max \left\{ a_5, \frac{\lambda_{C_1} SI}{B_5 (H + I)} \right\} \right\} \text{ and} \\ u_6^* &= \min \left\{ b_6, \max \left\{ a_6, \frac{\lambda_{C_2} I^2}{B_6 (H + I)} \right\} \right\}. \end{aligned} \quad (20)$$

The proof can be found in Appendix D.

5. NUMERICAL RESULTS

The parameter values applied to generate our simulations are listed in the table in Appendix A. The initial conditions of the simulations are based on the Philippines' H5N6 outbreak report (OIE 2020). We set $S(0) = 407\,837$, $I(0) = 73\,360$, $T(0) = 0$, $R(0)$, and the total population of birds $N(0) = 481\,197$.

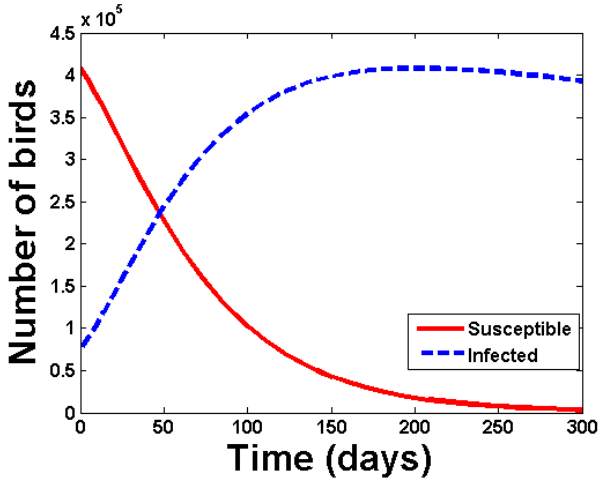

Figure 6: Simulation results showing the transmission dynamics of H5N6 in the Philippines with no intervention strategy. We use initial conditions and parameter values as follows: $S(0) = 407\,837$, $I(0) = 73\,360$, $\Lambda = \frac{2060}{365}$, $\mu = 3.4246 \times 10^{-4}$, $\beta = 0.025$, $H = 180\,000$, $\delta = 4 \times 10^{-4}$.

Previous studies suggested that the basic reproduction number for the presence of avian influenza without applying any intervention strategy was $\mathcal{R}_A = 3$ (Mills *et al.* 2004, Ward *et al.* 2009). We consider density-dependent transmission, where the contact between birds increases as the poultry population increases (Roche *et al.* 2009). We have calculated the transmissibility of the disease ($\beta = 0.025$) based on (5) with $\mathcal{R}_A = 3$, and fixed values of Λ (birth rate), μ (natural death rate), δ (disease induced death rate) and H (half-saturation constant). Without any control strategy, avian influenza will become endemic in the poultry population as shown in Figure 6. After 50 days, the population of the infected poultry exceeds that of susceptible poultry, with all birds eventually infected or dead.

5.1 Confinement with treatment strategy

Isolation of infected birds and application of treatment is a potential strategy to hinder an outbreak and reduce further spread of infection in the population. Figures 7–9 illustrate the effects of applying optimal control to the isolation-treatment strategy under different approaches. In Figure 7, we investigate the effects of varying the weight constant B_1 and B_2, which represents the relative cost of implementing isolation and treatment controls, respectively. Figure 8 portrays the difference between using a constant parameter and optimal control in describing the spread of infection using the isolation-treatment strategy. Figure 9 shows the disparity of using both isolation and treatment to using only one control measure.

As the relative cost of implementing isolation control B_1 and treatment control B_2 increases, slightly lower isolation and treatment rates are utilized, as illustrated in Figure 7. As we increase B_1 and B_2, the population of the susceptible birds decreases (see Figure 7A) while the population of the infected birds increases (as shown in Figure 7B). Isolated birds increase significantly in the first six days, then decline afterward due to treatment, as portrayed in Figure 7C. Increasing the cost of treatment leads to slower increase of recovered birds (Figure 7D) and slower decline of isolated birds (Figure 7C). We can observe that when we have lower values for B_1 and B_2, the susceptible population has a slower decline, there are fewer infected and isolated birds, and recovered birds increase faster. Thus, we consider $B_1, B_2 = 500{,}000$. Moreover, it can be observed that cheaper cost controls B_1 and B_2 (Figures 7A–D) should be administered at higher rates of u_1 and u_2 (shown in Figures 7E–F).

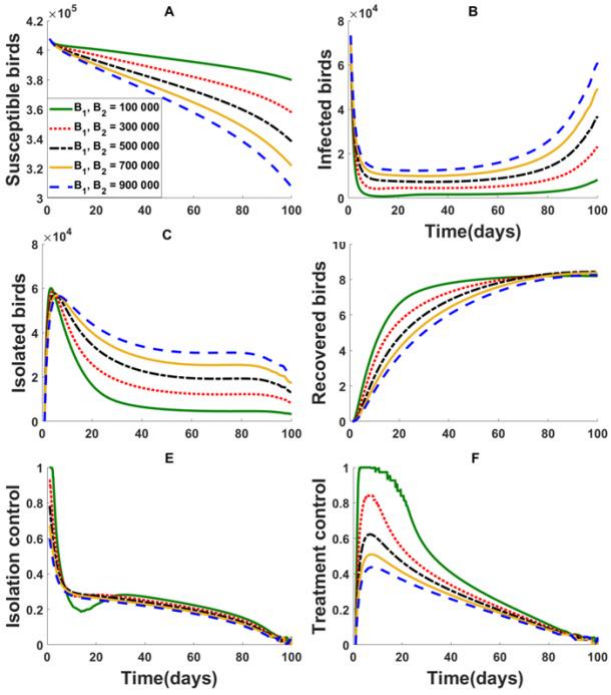

Figure 7: Application of isolation-treatment strategy with optimal control to the population of susceptible (A), infected (B), isolated (C) and recovered (D) birds along with isolation control (E) and treatment control (F) for varying values of B_i, for $i = 1, 2$, from 100 000 to 900 000 birds.

With optimal control, we can possibly prevent the spread of H5N6 in the poultry population, as demonstrated in Figure 8. The red dashed line (without optimal control) is a simulation of the isolation-treatment model (2) where we represent the isolation rate and the proportion of successfully recovered birds by a constant parameter. The blue solid line (with optimal control) is a simulation of isolation-treatment model (12) where control parameters $u_1(t)$ and $u_2(t)$ are included. In Figure 8A, the susceptible population declines slower under optimal control compared to using a constant parameter. This is due to rapid isolation of infected birds triggering the surge in Figure 8C with 78% isolation at the beginning, as seen in Figure 8E. It also has a faster increase in the recovered population, with 843,600 birds compared to 73,340 birds without optimal control within 100 days, as portrayed in Figure 8D. Application of optimal controls $u_1^*(t)$ and $u_2^*(t)$ in the susceptible, infected, isolated and recovered population is clearly better than using constant parameter (Figure 8). We can observe a slower decline of susceptible birds, an initial reduction in infected birds and a delayed increase in infection. More infected birds are isolated (Figure 8C), and we have a higher number of birds that will

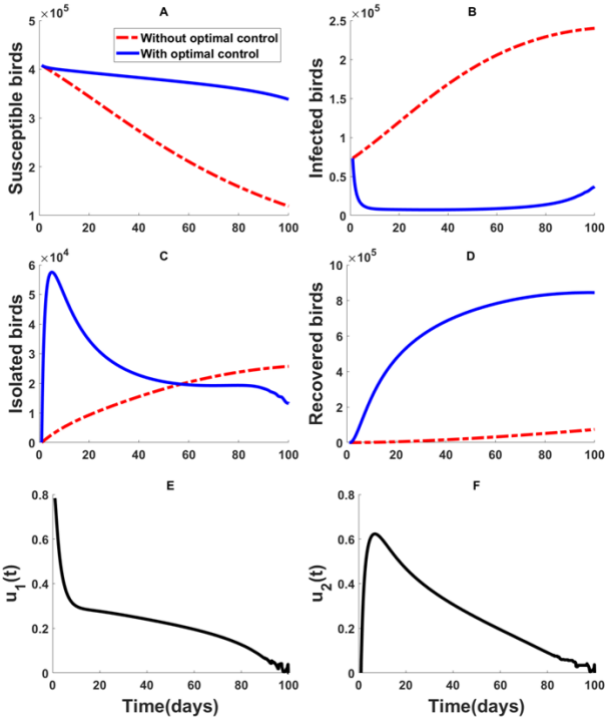

Figure 8: Applying isolation-treatment strategy with optimal control (blue solid line) and without optimal control or using constant parameter (red dashed line) in the population of susceptible (A), infected (B), isolated (C) and recovered (D) birds. Optimal-control values for isolation control u_1 (E) and treatment control u_2 (F) over 100 days.

recover after going through isolation (Figure 8D). Thus, using optimal control illustrated a more appropriate representation of implementing isolation-treatment strategy in controlling an outbreak.

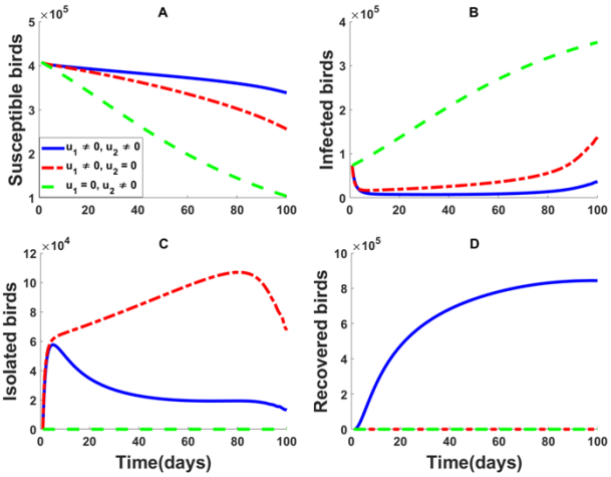

Figure 9: Isolation-treatment strategy with the optimal approach and with consideration of using both isolation and treatment control (blue solid line), using isolation control only (red dashed line), and using treatment only (green dashed line) to the population of susceptible (A), infected (B), isolated (C) and recovered (D) birds.

It is evident that using isolation together with treatment showed better results in all populations compared to implementing isolation alone or treatment alone, as depicted in Figure 9. In applying both controls, the susceptible populations decrease slowly; infected birds are eliminated from the poultry population; and isolated birds increase within 5 days, and then decrease afterward, which is due to releasing of birds from isolation. In reality, treatment can only be applied to birds that have been identified as infected. In the isolation-treatment

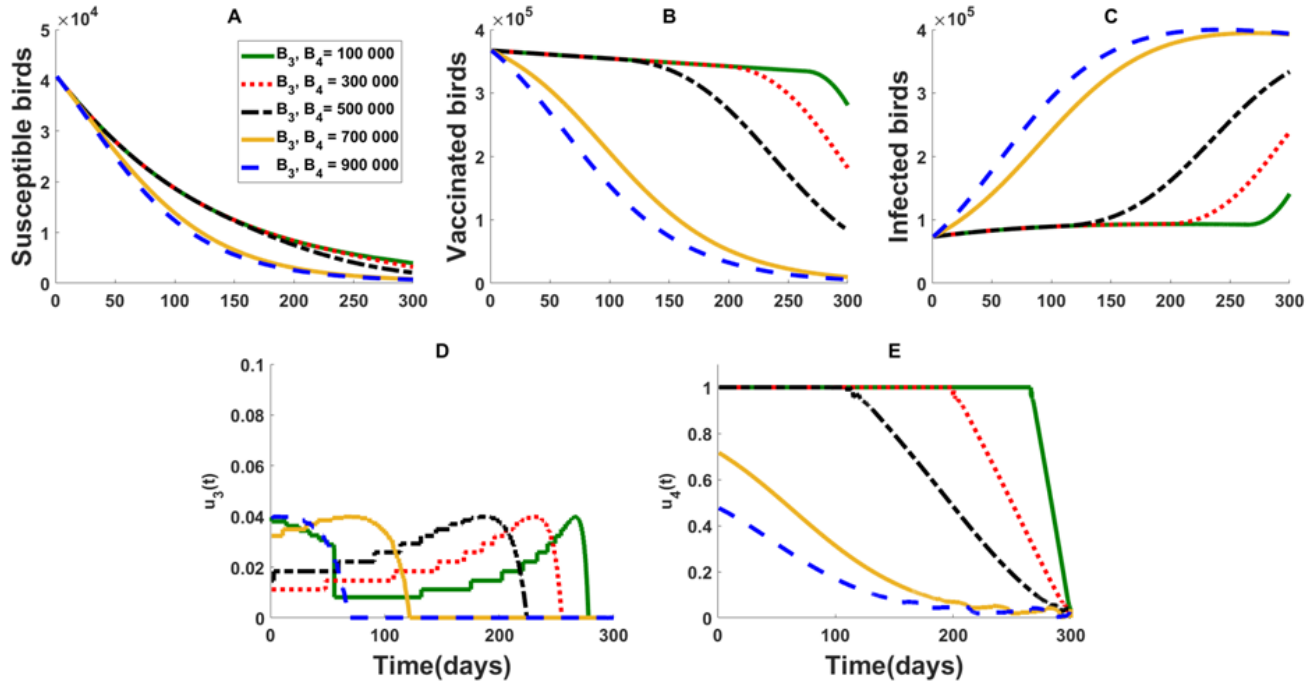

Figure 10: Application of vaccination strategy with optimal control to the population of susceptible (A), vaccinated (B) and infected (C) birds and the increased vaccination coverage (D) and the vaccine-efficacy control (E) with varying values of B_i, for $i = 3,4$, from 100 000 to 900 000 birds.

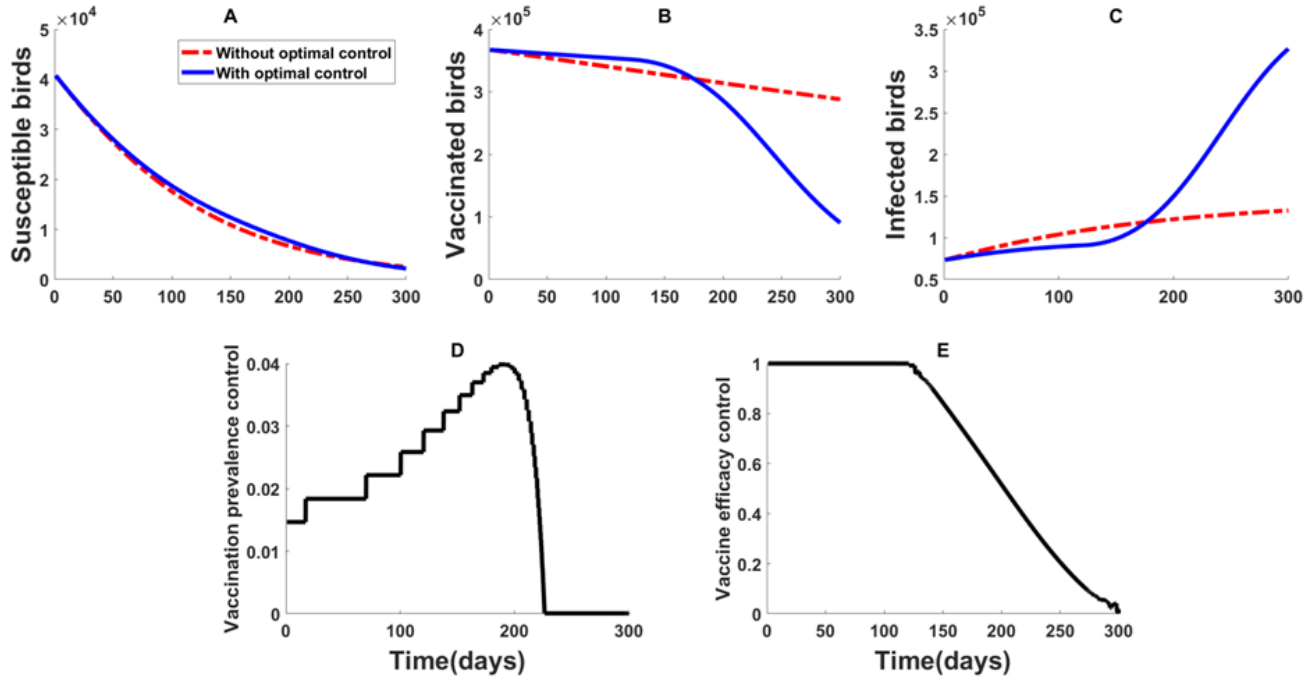

Figure 11: Applying the vaccination strategy with optimal control (blue solid line) and without optimal control or using constant parameter (red dashed line) in the population of susceptible (A), vaccinated (B) and infected (C) birds. Optimal-control values for vaccination prevalence control u_3 (D) and vaccine efficacy control u_4 (E) over 300 days.

model, treatment cannot be performed without isolation. Hence, the continuous increase in the infected population if $u_1 = 0$ and $u_2 \neq 0$ (represented by the green line in Figure 9). Isolated birds will transfer to either the infected or recovered population, depending on the effect of treatment. Without treatment ($u_1 \neq 0$ and $u_2 = 0$), isolated birds increase continuously then decrease after 85 days where the birds transfer to the infected population, as illustrated by the red line in Figures 9B–C. Applying isolation alone will reduce the infected population and prevent possible transmission of the disease to the susceptible population. However, due to the absence of treatment, birds will be released from isolation even though they are still infectious. This results in a rapid increase of the infected population after 85 days, as represented by the red line in Figure 9B. Our result suggests that isolation of infected birds without applying treatment is not sufficient to prevent the spread of H5N6 in the population.

5.2 Immunization strategy

Next, we consider immunizing the poultry population via a vaccine. Figure 10 illustrates the outcome of varying the relative cost of performing vaccination implementation control B_3 and vaccine efficacy control B_4. In Figure 11, we portray the comparison using fixed control (red dashed line) and optimal control (blue solid line).

In Figure 10, we observe that varying the relative costs (B_3 and B_4) of implementing the controls (u_3 and u_4) significantly

affects the spread of H5N6 in the vaccinated population. As we increase the relative costs, the vaccine efficacy decreases (Figure 10E), and this makes the vaccinated population vulnerable to acquiring H5N6. As shown in Figure 10D, the effects of varying the relative costs to vaccination control is very close to zero (the control ranges from 0 to 0.04), and it has a minimal effect in the spread of the virus in the population. We can observe that the changes in the vaccine efficacy (Figure 10E) greatly affect the curves in the vaccinated and infected population (Figures 10B–C). As the relative cost of the vaccine efficacy increases, the value of u_4 is lowered. Lower vaccine efficacy leads to rapid decline in the number of vaccinated birds and hence an increase in the infected population.

Through the application of optimal control, we can observe that the diminishing effectiveness of the vaccine results in the spread of infection in the vaccinated population, as depicted in Figure 11. After 120 days, the vaccine efficacy starts to decline, causing vaccinated birds to acquire the disease. Simulations shown in Figures 10–11 contribute to our understanding that immunizing the poultry population is not sufficient to prevent an outbreak. In using an optimal-control approach, we see that a successful immunization strategy highly depends on developing an effective vaccine. Note that, for the vaccination strategy, the cheapest vaccination is administered at a higher rate of vaccine efficacy control u_4 (shown in Figure 11).

5.3 Depopulation strategy

We obtain simulations for applying a modified culling strategy that targets infected birds as well as high-risk susceptible birds that are in contact with infected birds. Figure 12 compares the difference in outcomes of applying optimal control versus fixed control. Figure 13 depicts the effect of changing the relative cost of implementing the culling strategy for susceptible and infected populations. In Figure 14, we investigate the discrepancies in applying the modified culling strategy for culling both susceptible and infected birds, culling only susceptible birds and culling only the infected birds.

Integrating optimal control into a culling strategy results in a lower number of susceptible and infected birds compared to using a constant value, as portrayed in Figure 12. With optimal control, intensive culling occurred during the first 30 days of outbreak then slowed down over time. The decline in the numbers of both susceptible and infected birds occurs faster when optimal control is applied. In Figures 12A–B, 88% of susceptible birds and 63% of infected birds were culled within 30 days to prevent the spread of H5N6 avian influenza virus. After 100 days, there are only 4% susceptible birds and 11% infected birds left. Our optimal-control results suggest that culling of susceptible and infected birds must be implemented rigorously in the first 30 days of the outbreak to prevent further spread of the infection.

Even though the relative cost of culling increases for both susceptible and infected populations, we were able to control the outbreak and prevent further increase in the number of infected birds, as illustrated in Figure 13. We have lower values of culling controls for susceptible and infected populations (u_5 and u_6, respectively) when the relative cost of implementation increases, as depicted in Figures 13C–D. Thus, the higher cost of implementation of culling will result a higher number of susceptible birds but also more infected birds. Hence, varying the relative cost B_5 and B_6 from 100,000 to 900,000 will not affect the effectiveness of culling in preventing the spread of the H5N6 in the poultry population.

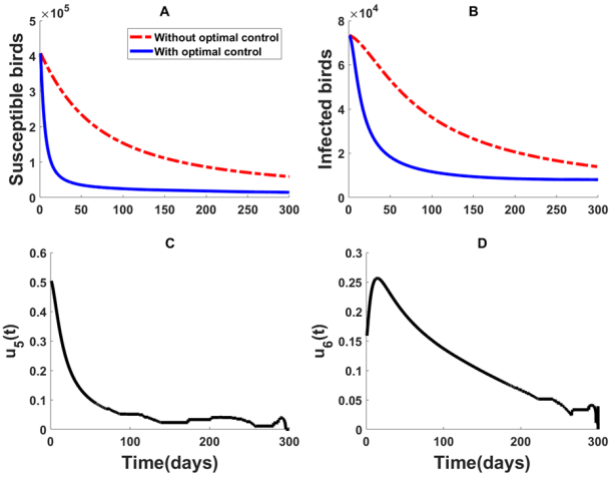

Figure 12: Implementing the culling strategy with optimal control (blue solid line) and without optimal control or using constant parameter (red dashed line) in the population of susceptible (A) and infected (B) birds. Optimal-control values of culling frequency control for susceptible (C) and infected (D) birds over 300 days.

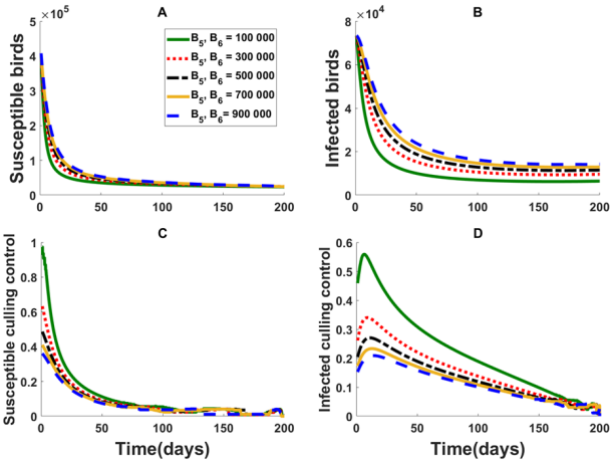

Figure 13: Application of culling strategy with optimal control to the population of susceptible (A) and infected (B) birds and susceptible-culling control (C) and infected-culling control (D), with varying values of B_i, for $i = 5, 6$, from 100 000 to 900 000 birds.

Administering a culling strategy for both susceptible and infected birds is more effective than culling only the infected birds, as indicated in Figure 14. Looking at the blue dashed line of Figure 14A, we have more susceptible birds if we cull only the infected population, but, as shown in Figure 14B, the infected population increases afterward. This implies that culling only the infected population is not enough to stop the spread of infection. We can infer that culling only the infected population can be successful if we can entirely eradicate the infected population. Currently, we cannot easily identify infected birds from the poultry population. Culling both susceptible and infected birds may lead to near eradication of the infected population, and due to the low number of susceptible birds, further spread of H5N6 would not be possible. Thus, culling both susceptible and infected birds is necessary to eliminate the spread of infection in the poultry population.

In the 2017 Central Luzon H5N6 outbreak, it cost the country's poultry industry 2.3 billion pesos with around 160,000 infected poultry (Simeon, 2017). There is insufficient data for the actual cost of implementation of each strategy per poultry. Henceforth,

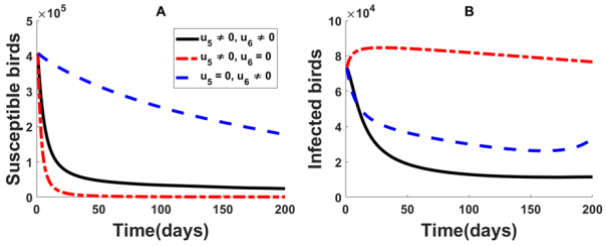

Figure 14: Simulation of culling strategy with the optimal approach and with consideration of using both susceptible culling control $u_5(t)$and infected culling control $u_6(t)$ (black solid line), using susceptible culling control $u_5(t)$ only (red dotted-dashed line) and using infected culling control $u_6(t)$ to the population of susceptible (A) and infected (B) birds.

in this study, we can only present an abstract concept of the cost (based on the number of infected birds) and compare the cost from each strategy. Among the three strategies, we concluded that the modified culling strategy is the cheapest with the least number of infected birds after 100 days. For future work, collaborations with engineers can be established to build the actual facilities and compute the cost per unit of poultry.

Table 1: Total cost of implementation and the number of infected birds after 100 days for each strategy.

Strategies	Total Cost	Infected birds after 100 days
Isolation-treatment	$5.0\text{x}10^4$	$3.7\text{x}10^4$ (reduced by 50%)
Vaccination	$2.8\text{x}10^5$	$8.9\text{x}10^4$ (increased by 22%)
Modified culling	$8.1\text{x}10^3$	$1.2\text{x}10^4$ (reduced by 84%)

6. DISCUSSION

Understanding and learning to control avian influenza is a crucial issue for many countries, especially in Asia. Avian influenza virus A (H5N6) is an emerging infectious disease that was reported in China in early May 2014 (Joob and Viroj 2015). In 2017, the Philippines reported an outbreak of H5N6 which resulted in a mass culling of 667,184 birds. After more than two years H5N6 reemerged, causing the depopulation of 12,000 quails (OIE 2020). Lee and Lao (2017) proposed intervention strategies against the spread H5N6 virus in the Philippines. They suggested poultry isolation strategy over vaccination strategy in reducing the number of infected birds.

There is limited study on the effects of isolation with treatment as a control strategy against the spread of avian influenza. Isolation is also used when adding new flocks of birds to the poultry farm in order to prevent possible transmission of disease to the current flock. We investigated the effects of isolation-treatment strategy as a promising policy in controlling an outbreak. We modified the isolation model of Lee and Lao (2017) and emphasize the role of treatment in utilizing this strategy. We focused on the impact of isolation control u_1 and treatment control u_2 in applying this strategy. Isolating infected birds is an effective measure to reduce the spread of H5N6 in the population, as claimed by Lee and Lao (2017). We followed up confinement by applying treatment during isolation, which turns out to have a significant role in applying confinement. Through our simulation in Figures 7–9, we showed that transmission of H5N6 virus in the poultry population can be reduced by isolating at least 78% of the infected birds. In addition, at least 62% of the isolated birds must successfully recover from the infection within the first week.

Using optimal-control theory, we showed that the success of vaccination is highly dependent on the effectiveness of the chosen vaccine. A less-effective vaccine will make vaccinated birds vulnerable to acquiring the virus. Vectormune AI is a rHVT-H5 vaccine which provides 73% protection against AIV H5 type (Kilany *et al.* 2014). In the study of Cornelissen and colleagues (2012), the NDV-H5 vaccine induced 80% immunity to chicken against H5N1. A fowlpox vector vaccine TROVAC-H5 protected chickens against avian influenza for at least 20 weeks (Bublot *et al.* 2006). Despite effective vaccines, there is a possibility for the effectiveness of the vaccine to decline over time, so we suggest that vaccination should be implemented together with other intervention strategies in preventing the spread of H5N6 in the population.

Mass culling of birds is the current policy used when detecting an outbreak of avian influenza, which is applied to the infected farm and a short radius around the infected premises (OIE, 2020). We considered a modified culling strategy, as suggested in the study of Gulbudak and Martcheva (2013), which focused on culling infected birds as well as high-risk susceptible birds that are in contact with infected birds. We showed that culling only the infected birds is not enough to contain the spread of H5N6. Instead, culling 78% of susceptible birds and at least 63% of infected birds within 30 days can prevent an outbreak and avoid further transmission of the virus in the poultry population.

The modified culling strategy has the cheapest implementation cost with the least number of infected birds after 100 days. It should be implemented if rapid eradication of the outbreak is necessary, with the understanding that the consequence is losing a large number of birds in the process. On the other hand, if we aim to conserve the poultry population, then the isolation with treatment strategy will potentially prevent the outbreak with most of the birds recovered from the infection. This strategy can be achieved through a rapid isolation of infected birds and a reliable treatment policy. Conversely, vaccination should be implemented only with other intervention strategies.

Note that we used three different models for each strategy, which limits our comparison of the three control strategies. Future work will consider combinations of strategies and conduct numerical continuation studies to track both stable and unstable steady states and bifurcation points in the systems in order to gain better understanding and new discoveries of the overall dynamics of the epidemiological systems.

Using optimal-control theory gives us a better understanding of H5N6 outbreak prevention. By applying optimal control to different strategies against H5N6, we have illustrated the effects of each policy, together with its respective implementation cost. Every intervention strategy against H5N6 has advantages and disadvantages, but proper execution and appropriate application is a significant factor in achieving a desirable outcome.

ACKNOWLEDGMENTS

Lucido acknowledges the support of the Department of Science and Technology-Science Education Institute (DOST-SEI), Philippines for the ASTHRDP Scholarship grant together with the Career Incentive Program (CIP). Lao holds research fellowship from De La Salle University. Smith? is supported by an NSRC Discovery Grant. For citation purposes, please note that the question mark in "Smith?" is part of his name. We thank the anonymous reviewers whose comments helped improve and clarify this manuscript.

CONFLICTS OF INTEREST

Lucido, Smith? and Lao declare that they have no conflict of interest.

REFERENCES

Agusto FB. Optimal isolation control strategies and cost-effectiveness analysis of a two-strain avian influenza model. Biosys2013; 113 (3):155–164.

Bi Y, Chen Q, Wang Q, Shi W, Liu D, Gao GF. Genesis, Evolution and Prevalence of H5N6 Avian Influenza Viruses in China. Cell Host Microbe 2016; 20 (6):810–821.

Bublot M, Pritchard N, Swayne DE, Selleck P, Karaca K, Suarez D, Audonnet J-C, Mickle T. Development and use of fowlpox vectored vaccines for avian influenza. *Ann N Y Acad Sci*. 2006;1081:193-201.

Butler D. Vaccination will work better than culling, say bird flu experts. Nature 2005; 434:810.

Capasso V, Serio G. A generalization of the Kermack-McKendrick deterministic epidemic model. Math Biosci1978; 42 (1):43–61.

Chen H. Avian influenza vaccination: the experience in China. Revue Scientifique et Technique de l'OIE2009; 28 (1):267–274.

Chong NS, Tchuenche JM, Smith? RJ. A mathematical model of avian influenza with half-saturated incidence. Theory Biosci2014; 133 (1):23–38.

Cornelissen LA, Leeuw OS, Tacken MG, Klos HC, Vries RR, Boer-Luijtze EA, Zoelen-Bos EA, Rigter A, Rottier PJ, Moormann RJ, Haan CA. Protective efficacy of Newcastle disease virus expressing soluble trimeric hemagglutinin against highly pathogenic H5N1 influenza in chicken and mice. PLoS ONE 2012; 7(8):1–11.

FAO. The Global Strategy for Prevention and Control of H5N1 Highly Pathogenic Avian Influenza, 2007.

Fleming W, Rishel R. Optimal deterministic and stochastic control. Springer, 1975.

Gulbudak H, Martcheva M. Forward hysteresis and backward bifurcation caused by culling in an avian influenza model. MathBiosci2013; 246 (1):202–212.

Gulbudak H, Ponce J, Martcheva M. Coexistence caused by culling in a two-strain avian influenza model. Preprint, J Biol Dynamics 2014; 367 (1):1–22.

Gumel AB. Global dynamics of a two-strain avian influenza model. Int J of Comp Math 2009; 86 (1):85–108.

Joob B, Viroj W. H5N6 influenza virus infection, the newest influenza. Asian Pac J Trop Biomed 2015; 5 (6): 434–437.

Jung E, Iwami S, Takeuchi Y, Jo T-C. Optimal control strategy for prevention of avian influenza pandemic. J Theor Biol. 2009; 260(2):220–229.

Kilany W, Dauphin G, Selim A, Tripodi A, Samy M, Sobhy H, VonDobschuetz S, Safwat M, Saad M, Erfan A, Hassan M, Lubroth J, Jobre Y. Protection conferred by recombinant turkey herpesvirus avian influenza (rHVT-H5) vaccine in the rearing period in two commercial layer chicken breeds in Egypt. Avian Pathol. 2014; 43:6:514-523.

Kim S, de los Reyes AA, Jung E. Mathematical model and intervention strategies for mitigating tuberculosis in the Philippines. J Theor Biol. 2018; 443:100–112.

Lee H, Lao A. Transmission dynamics and control strategies assessment of avian influenza A (H5N6) in the Philippines. Infec Dis Model2018; 3:35–59.

Liu S, Ruan S, Zhang X. Nonlinear dynamics of avian influenza epidemic models. Math Biosci 2017; 283:118–135.

Liu Z, Fang C-T. A modeling study of human infections with avian influenza A H7N9 virus in mainland China. Int J Infect Dis 2015; 41:73–78.

Mills CE, Robins JM, Lipsitch M. Transmissibility of 1918 pandemic influenza. Nature 2004; 432 (7019):904–906.

OIE. World Animal Health Information System, 2020.

Okosun KO, Smith? R. Optimal control analysis of malaria–schistosomiasis co-infection dynamics. Math BiosciEng 2017; 14:377–405.

Pontryagin LS, Boltyanskii V, Gamkrelidze R, Mishchenko E. Mathematical Theory of Optimal Processes. CRC Press Book, 1986.

Roche B, Lebarbenchon C, Gauthier-Clerc M, Chang C-M, Thomas F, Renaud F, van der Werf S, Guegan J-F. Water-borne transmission drives avian influenza dynamics in wild birds: The case of 2005-2006 epidemics in the Camargue Area. Infect GenetEvol2009; 9:800-805.

Shi Z, Zhang X, Jiang D. Dynamics of an avian influenza model with half-saturated incidence. ApplMath Comput 2019; 355:399–416.

Simeon, L. (2017, September 08). Avian flu poultry ban partially lifted. Retrieved August 23, 2020, from https://www.philstar.com/headlines/2017/08/22/1731805/avian-flu-poultry-ban-partially-lifted.

Teng Y, Bi D, Guo X, Hu D, Feng D, Tong Y. Contact reductions from live poultry market closures limit the epidemic of human infections with H7N9 influenza. J Infect 2018; 76 (3):295–304.

van den Driessche P, Watmough J, Reproduction numbers and sub-threshold endemic equilibria for compartmental models of disease transmission. Math Biosci2002; 180:29–48.

Ward MP, Maftei D, Apostu C, Suru A. Estimation of the basic reproductive number (R0) for epidemic, highly pathogenic avian influenza subtype H5N1 spread. Epi Infect 2009; 137 (2):219–226.

WHO. Influenza (Avian and other zoonotic), 2020.

Appendix A. Variables and parameters

Here, we describe each variable and parameter that we used in each model.

Notation	Description or Label
$S(t)$	Susceptible birds
$I(t)$	Infected birds
$T(t)$	Isolated birds
$R(t)$	Recovered birds
$V(t)$	Vaccinated birds
$N(t)$	Total bird population
Λ	Constant birth rate of birds
μ	Natural death rate of birds
β	Rate at which birds contract avian influenza
H	Half-saturation constant for birds
δ	Additional disease death rate due to avian influenza
p	Proportion of vaccinated poultry
ϕ	Efficacy of the vaccine
ω	Isolation rate of identified infected birds
γ	Releasing rate of birds from isolation
f	Proportion of recovered birds from isolation
c_s	Culling frequency for susceptible birds
c_i	Culling frequency for infected birds
$\tau_s(I)$	Culling rate of susceptible birds
$\tau_i(I)$	Culling rate of infected birds

The initial conditions are based on Philippine Influenza A (H5N6) outbreak report given by the OIE (2020): $S(0) = 407\,837$ and $I(0) = 73\,360$. We calculated transmissibility of the disease ($\beta = 0.025$) using the basic reproduction number $\mathcal{R}_A$ in (5) and equating it to 3, the value of the basic reproduction number of AIV without intervention (Mills *et al.* 2004, Ward *et al.* 2009).We calculated parameter values that reduce the basic reproduction number below one and control the spread of AIV in the poultry population.

Definition	Symbol	Value	Source
Constant birth rate of birds	Λ	$\frac{2060}{365}$per day	(Chong *et al.* 2013)
Natural mortality rate	μ	3.4246×10^{-4}per day	(Liu *et al.* 2017)
Transmissibility of the disease	β	0.025per day	Calculated[1]
Half-saturation constant for birds	H	180 000birds	(Lee and Lao 2018)
Disease-induced death rate of poultry	δ	4×10^{-4}per day	(Liu *et al.* 2017)
Proportion of vaccinated poultry	p	0.50	Calculated[1,2]
Vaccine efficacy	ϕ	0.90	Calculated[1,2]
Waning rate of the vaccine	ω	0.00001per day	Calculated[1]
Isolation rate of identified infected birds	ψ	0.01per day	Calculated[1,2]
Release rate of birds from isolation	γ	0.09per day	Calculated[1]
Proportion of recovered birds from isolation	f	0.5	Calculated[1,2]
Culling frequency for susceptible birds	c_s	$\frac{1}{60}$per day	Estimated[2]
Culling frequency for infected birds	c_i	$\frac{1}{7}$per day	Estimated[2]

[1]Calculated means we compute this value using the basic reproduction number

[2]These values will become the controls when optimal-control theory is applied.

Appendix B. Non-existence of backward bifurcation

Appendix B.1. Vaccination

In showing that a backward bifurcation does not exist for the vaccination model, we solve for $I_V^* = \frac{-b \pm \sqrt{b^2-4ac}}{2a}$ such that

$$\begin{aligned} a &= -(\mu+\delta)[\mu\beta(1-\phi) + (\mu+\omega)(\mu+\beta) + \beta^2(1-\phi)], \\ b &= \beta^2\Lambda(1-\phi) + \mu H(\mu+\delta)(\mu+\omega)(\mathcal{R}_V - 1) \\ &\quad - H(\mu+\delta)[\mu\beta(1-\phi) \\ &\quad + (\mu+\beta)(\mu+\omega)], \\ c &= \mu H^2(\mu+\delta)(\mu+\omega)(\mathcal{R}_V - 1). \end{aligned} \qquad (B.1)$$

Theorem B.1. The vaccination model (3) has no endemic equilibrium when $\mathcal{R}_V \leq 1$ and has a unique endemic equilibrium when $\mathcal{R}_V > 1$.

Proof. We obtain two possible endemic equilibria $E_{V_1}^*$ and $E_{V_2}^*$ for the vaccination model. From $(B.1)$, we establish the relationship between $\mathcal{R}_V$ and c such that

$$\mathcal{R}_V > 1 \Leftrightarrow c > 0 \quad \mathcal{R}_V = 1 \Leftrightarrow c = 0 \quad \mathcal{R}_V < 1 \Leftrightarrow c < 0$$

From $(B.1)$, it is clear that $a < 0$. Consider the cases when $c > 0$, when $b > 0$ and $c = 0$ or $b^2 - 4ac = 0$, and when $c < 0, b > 0$, and $b^2 - 4ac > 0$.

Case 1: $c > 0$

When $c > 0$, we have $\mathcal{R}_V > 1$. Since $a < 0$, it follows that

$$I_{V_1}^* = \frac{-b+\sqrt{b^2-4ac}}{2a} < 0$$

$$I_{V_2}^* = \frac{-b-\sqrt{b^2-4ac}}{2a} > 0.$$

When $\mathcal{R}_V > 1$ the infected population $\left(I_{V_1}^*\right)$ of the endemic equilibrium $\left(E_{V_1}^*\right)$ does not exist, and we have a unique endemic equilibrium $E_{V_2}^*$.

Case 2: $b > 0$ and either $c = 0$ or $b^2 - 4ac = 0$
Given that $b > 0$, we consider the case when $c = 0$ and when $b^2 - 4ac = 0$.

Case 2A: $c = 0$
Since $c = 0$, it follows that $I_{V_1}^* = 0$ and $I_{V_2}^* > 0$. Note that $I_{V_1}^* = 0$ leads to the DFE. Hence, if $b > 0$ and $c = 0$, then $I_{V_2}^* > 0$, and we have a unique endemic equilibrium $E_{V_2}^*$.

Case 2B: $b^2 - 4ac = 0$
Considering that $b^2 - 4ac = 0$, it follows that $I_{V_1}^* = I_{V_2}^*$ and $I_{V_1}^*, I_{V_2}^* > 0$. Thus, if $b > 0$ and $b^2 - 4ac = 0$, then we have a unique endemic equilibrium $E_{V_1}^* = E_{V_2}^*$.

Case 3: $c < 0, b > 0$, and $b^2 - 4ac > 0$.

From the assumption that $a < 0$ and $c < 0$, it follows that

$$I_{V_1}^* = \frac{-b+\sqrt{b^2-4ac}}{2a} > 0 \qquad I_{V_2}^* = \frac{-b-\sqrt{b^2-4ac}}{2a} > 0$$

Thus, we have two endemic equilibria $E_{V_1}^*$ and $E_{V_2}^*$, which implies that a backward bifurcation may possibly occur whenever $c < 0, b > 0$, and $b^2 - 4ac > 0$.

However, given the values of b and c, we can show that when $c < 0$, we cannot obtain $b > 0$, which we prove by contradiction. Suppose that $c < 0$. By definition of p and ϕ, the value of both parameters ranges from 0 to 1. From $(B.1)$, it follows that $\Lambda\beta < \frac{\mu H \Delta}{\Theta}$, where we define $\Theta = (\mu + \omega - p\mu\phi)$ and $\Delta = (\mu+\delta)(\mu+\omega)$.

Using $(B.1)$ with $b > 0$, we get $\Lambda\beta^2(1-\phi) + \Lambda\beta\Theta > 2\mu H\Delta + \beta H\Delta + \mu H\beta(\mu+\delta)(1-\phi)$. By simplifying, we obtain

$$\frac{\mu\beta(\mu+\omega)(1-\phi)}{\Theta} > \mu(\mu+\omega) + \beta(\mu+\omega) + \mu\beta(1-\phi). \qquad (B.2)$$

In both extreme values of ϕ, it follows that

$$0 > \mu(\mu+\omega) + \beta(\mu+\omega).$$

Since $\mu, \omega, \beta \geq 0$, it implies that $\mu(\mu+\omega) + \beta(\mu+\omega) \geq 0$, and we have a contradiction. Results above suggest that two endemic equilibria do not exist when $\mathcal{R}_V < 1$, since the condition $c < 0$, $b > 0$, and $b^2 - 4ac > 0$, cannot be satisfied. From Cases 1 to 3, it is evident that the vaccination model has no endemic equilibrium when $\mathcal{R}_V < 1$ and a unique endemic equilibrium when $\mathcal{R}_V \geq 1$.

Appendix B.2. Culling

To show that a backward bifurcation does not exist for the culling model, we solve for $I_C^* = \frac{-b \pm \sqrt{b^2-4ac}}{2a}$ such that

$$\begin{aligned} a &= -(\mu+\delta+c_i)(\mu+c_s+\beta), \\ b &= \mu H(\mu+\delta)(\mathcal{R}_C - 1) - c_i\mu H - H(\mu+\delta)(\mu+c_s+\beta), \\ c &= \mu H^2(\mu+\delta)(\mathcal{R}_C - 1). \end{aligned} \qquad (B.3)$$

Theorem B.2. The culling model (4) has no endemic equilibrium when $\mathcal{R}_C < 1$ and has a unique endemic equilibrium when $\mathcal{R}_C > 1$.

Proof. We obtain two possible endemic equilibria, $E_{C_1}^*$ and $E_{C_2}^*$, for the culling model. From $(B.3)$, $a < 0$, and we consider cases where $\mathcal{R}_C < 1$, $\mathcal{R}_C = 1$, and $\mathcal{R}_C > 1$.

Case 1: $\mathcal{R}_C < 1$
When $\mathcal{R}_C$ is below unity, it follows that $c < 0$ and $b < 0$. Given that $a < 0$ and $c < 0$, we have

$$I_{C_1}^* = \frac{-b+\sqrt{b^2-4ac}}{2a} < 0 \quad I_{C_2}^* = \frac{-b-\sqrt{b^2-4ac}}{2a} < 0.$$

Thus, in our case when $\mathcal{R}_C < 1$, we have no endemic equilibrium.

Case 2: $\mathcal{R}_C = 1$

When $\mathcal{R}_C = 1$, we have $c = 0$ and $a < 0$. It follows that $\sqrt{b^2-4ac} = b$. Since $a < 0$, we have

$$I_{C_1}^* = \frac{-b+b}{2a} = 0 \qquad I_{C_2}^* = \frac{-b-b}{2a} < 0.$$

Hence, when $\mathcal{R}_C = 1$, we have no endemic equilibrium.

Case 3: $\mathcal{R}_C > 1$
When $\mathcal{R}_C$ is above the unity, it follows that $c > 0$. Given that $a < 0$ and $c > 0$, we have

$$I_{C_1}^* = \frac{-b + \sqrt{b^2 - 4ac}}{2a} < 0 \qquad I_{C_2}^* = \frac{-b - \sqrt{b^2 - 4ac}}{2a} > 0.$$

Hence, when $\mathcal{R}_C > 1$, we have $I_{C_2}^* > 0$ and a unique endemic equilibrium $E_{C_2}^*$.

Appendix C. Proof of Theorem 4.2

Proof. The existence of optimal control (u_3^*, u_4^*) is given by the result of Fleming and Rishel (1975). Boundedness of the solution of (3) shows the existence of a solution for the system. We have nonnegative values for the controls and state variables. In our minimizing problem, we have a convex integrand for J_V with respect to (u_3, u_4). By definition, the control set is closed, convex and compact, which shows the existence of optimality solutions in our optimal system. We use Pontryagin's Maximum Principle to obtain the adjoint equations and transversality conditions. We differentiate the Hamiltonian (16) with respect to the corresponding state variables as follows:

$$\frac{d\lambda_{V_1}}{dt} = -\frac{\partial H_V}{\partial S}, \qquad \frac{d\lambda_{V_2}}{dt} = -\frac{\partial H_V}{\partial V}, \qquad \frac{d\lambda_{V_3}}{dt} = -\frac{\partial H_V}{\partial I},$$

with $\lambda_{V_i}(t_f) = 0$ where $i = 1, 2, 3$. Using the optimality condition

$\frac{\partial H_V}{\partial u_3} = B_3 u_3(t) - \lambda_{V_1}\Lambda + \lambda_{V_2}\Lambda = 0$ and
$\frac{\partial H_V}{\partial u_4} = B_4 u_4(t) + \lambda_{V_2}\frac{\beta VI}{H+I} - \lambda_{V_3}\frac{\beta VI}{H+I} = 0,$

we derive the optimal controls (17). We consider the bounds for the control and conclude the characterization for u_3^* and u_4^*

$u_3^* = \min\left\{1, \max\left\{0, \frac{(\lambda_{V_1} - \lambda_{V_2})\Lambda}{B_3}\right\}\right\}$ and
$u_4^* = \min\left\{1, \max\left\{0, \frac{(\lambda_{V_3} - \lambda_{V_2})\beta VI}{B_4(H+I)}\right\}\right\}.$

Appendix D. Proof of Theorem 4.3

Proof. Analagous to the previous proof, we differentiate the Hamiltonian (19) with respect to the corresponding state variables as follows:

$$\frac{d\lambda_{C_1}}{dt} = -\frac{\partial H_C}{\partial S}, \qquad \text{and} \qquad \frac{d\lambda_{C_2}}{dt} = -\frac{\partial H_C}{\partial I},$$

with $\lambda_{C_1}(t_f) = 0$ where $i = 1, 2$. We consider the optimality condition

$$\frac{\partial H_C}{\partial u_5} = B_5 u_5(t) - \frac{\lambda_{C_1} SI}{H+I} = 0 \quad \text{and} \quad \frac{\partial H_C}{\partial u_6} = B_6 u_6(t) - \frac{\lambda_{C_2} I^2}{H+I} = 0,$$

to derive the optimal controls (20). We consider the bounds of the controls and get the characterization for u_5^* and u_6^*

$u_5^* = \min\left\{1, \max\left\{0, \frac{\lambda_{C_1} SI}{B_5(H+I)}\right\}\right\}$ and
$u_6^* = \min\left\{1, \max\left\{0, \frac{\lambda_{C_2} I^2}{B_6(H+I)}\right\}\right\}.$